대한기계학회 2001년도 춘계학술대회논문집 D pp. 97~103 KSME 01S409

Effects of Electrohydrodynamic Flow and Turbulent Diffusion on Collection Efficiency of an Electrostatic Precipitator with Cavity Walls

Seok Joo Park, Young Ok Park*, Sang Soo Kim** and Peter H. McMurry***

Key Words : Electrohydrodynamic flow, Turbulent diffusion, Collection efficiency, Electrostatic precipitator, Cavity wall.

Abstract

The effects of the electrohydrodynamic (EHD) flow and turbulent diffusion on the collection efficiency of a model ESP composed of the plates with a cavity were studied through numerical computation. The electric field and ion space charge density were calculated by the Poisson equation of the electrical potential and the current continuity equation. The EHD flow field was solved by the continuity and momentum equations of the gas phase including the electrical body force induced by the movement of ions under the electric field. The RNG k-ε model was used to analyze the turbulent flow. The particle concentration distribution was calculated from the convective diffusion equation of the particle phase. As the ion space charge increased, the particulate collection efficiency increased because the electrical potential increased over the entire domain in the ESP. The collection efficiency decreased and then increased, i.e. had a minimum value, as the EHD circulating flow became stronger when the electrical migration velocity of the charged particle was low. However, the collection efficiency decreased with the stronger EHD flow when the electrical migration of the particle was higher relatively. The collection efficiency of the model ESP increased as the turbulent diffusivity of the particle increased when the electrical migration velocity of the particle was low. However, the collection efficiency decreased for increasing the turbulent diffusivity when the electrical migration of the particle was higher relatively.

1. Introduction

An electrostatic precipitator (ESP) is a device for the collection of contaminated particles under the electrostatic force. The ESP consists of grounded collecting electrodes and corona discharge electrodes. The discharge and collecting electrodes with various complicated shapes have been developed to improve the performance of an ESP.

The fluid flow inside the ESP may be divided into the primary flow and secondary flow. The primary flow is the gas flow through the precipitator when the corona discharge is not occurred. It is also called the cross-flow. The secondary flow is the flow caused by the electrical migration of ions produced by the corona discharge. The secondary flow is also called the corona wind, ionic wind, or electric wind. The corona wind interacts with the cross-flow, so that it produces the complicated electrohydrodynamic (EHD) flow. The corona wind influences the particle behavior, especially for submicron particles in which the electrical migration velocity is small. The corona wind has been estimated to decrease the collection efficiency of a conventional wire – flat plate ESP. That is because the corona wind obstructs the movement of charged particles toward the collecting electrode and increases the turbulence level of gas flow (Kallio and Stock, 1992). However, few studies about the effect of EHD flow on the particle collection in the ESP composed of specific shaped plates have been attempted.

The performances of the flat plate – plate ESP, the wire – cylindrical tube ESP, or the wire – flat plate ESP have been known to be affected significantly by the turbulence condition of the cross-flow (Riehle and Löffler, 1995). The turbulence level at the inlet of ESP may be determined by the design of diffusers or baffles. The diffuser is used to make the gas flow entering the ESP uniform, and the baffle is used to support the long collecting plate and discharge wire. Most of them have reported that the collection efficiency of an ESP should greatly increase as the turbulence level of inlet cross-flow decreases.

In the present study, we estimated the effects of EHD flow and turbulent diffusion on the performance of a

* Korea Institute of Energy Research
** Korea Advanced Institute of Science and Technology
*** University of Minnesota

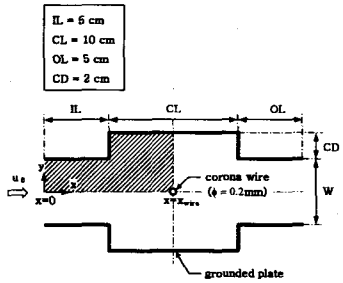

Figure 1. Geometry of model electrostatic precipitator.

model ESP (referred as 'a wire - cavity plate ESP' in the present study) through the numerical studies. As shown in Fig. 1, the simple geometry composed of the plates with a cavity (referred as 'cavity plate' in the present study) was used as the model ESP.

2. Governing Equations

The principal three fields, which are the electric field, the gas flow field, and the particle concentration field, are coupled one another in the ESP. The transport of ions by the air convection is insignificant in comparison of the electrical migration of ions under the Coulomb force in the conventional operating condition of the ESP (Yamamoto and Velkoff, 1981). So the fluid flow does not influence the electric field distribution. And low particle volume fraction is assumed in the present study, so that the one-way coupling may be applied to the gas particulate flow field (Elghobashi, 1994) and the effect of particle space charge on the electric field is negligible. Consequently, the electric field and ion space charge density is calculated, and then the fluid flow field is solved with the results of the electric field intensities and space charge densities. After the information about the electric field, space charge density, and fluid flow field are obtained, the particle concentration distribution in the ESP is calculated.

Steady-state two-dimensional fields are assumed to simplify the physical phenomena. The influence of the corona wire on the fluid flow and particle dynamic fields may be neglected since the diameter of the corona wire is much smaller than the geometric size of the ESP. And the inertia of particles in turbulent flow is negligible because the particle Stokes number is not important for the conventional flow condition of the ESP if the particle diameter is less than 10 μm (Leonard, 1982).

Dimensionless governing equations are expressed as follows:

Electric potential and current continuity equation

$$\frac{\partial^2 V^*}{\partial x^{*2}} + \frac{\partial^2 V^*}{\partial y^{*2}} = -\mathrm{Y}_0 \rho_c^*$$

$$\rho_c^{*2} = \frac{1}{\mathrm{Y}_0}\left(\frac{\partial \rho_c^*}{\partial x^*}\frac{\partial V^*}{\partial x^*} + \frac{\partial \rho_c^*}{\partial y^*}\frac{\partial V^*}{\partial y^*}\right)$$

Momentum equation of gas phase

$$u^*\frac{\partial u^*}{\partial x^*} + \upsilon^*\frac{\partial u^*}{\partial y^*} = -\frac{\partial p^*}{\partial x^*} + \frac{1}{\mathrm{Re}}\left(\frac{\partial^2 u^*}{\partial x^{*2}} + \frac{\partial^2 u^*}{\partial y^{*2}}\right) + \mathrm{N}_{\mathrm{EHD}}\rho_c^* E_x^*$$

$$u^*\frac{\partial \upsilon^*}{\partial x^*} + \upsilon^*\frac{\partial \upsilon^*}{\partial y^*} = -\frac{\partial p^*}{\partial y^*} + \frac{1}{\mathrm{Re}}\left(\frac{\partial^2 \upsilon^*}{\partial x^{*2}} + \frac{\partial^2 \upsilon^*}{\partial y^{*2}}\right) + \mathrm{N}_{\mathrm{EHD}}\rho_c^* E_y^*$$

Convective diffusion equation of particle phase

$$\frac{\partial}{\partial x^*}\left[\left(\frac{u^*}{\Omega_0} + E_x^*\right)n^*\right] + \frac{\partial}{\partial y^*}\left[\left(\frac{\upsilon^*}{\Omega_0} + E_y^*\right)n^*\right] = \frac{1}{\mathrm{Pe}_0}\left[\frac{\partial}{\partial x^*}\left(D_x^*\frac{\partial n^*}{\partial x^*}\right) + \frac{\partial}{\partial y^*}\left(D_y^*\frac{\partial n^*}{\partial y^*}\right)\right]$$

where Y_0, Re, $\mathrm{N}_{\mathrm{EHD}}$, Ω_0 and Pe_0 are the space charge parameter (Yabe *et al.*, 1978), the Reynolds number, the electrohydrodynamic number (Yamamoto and Velkoff, 1981), the electrical drift parameter (Riehle and Löffler, 1995) and the electrical Peclet number, respectively. Definitions and interpretations of these dimensionless parameters are as follows.

$$\mathrm{Y}_0 = \frac{\rho_{c0} d^2}{\varepsilon_0 V_0} = \frac{\text{electric field enhanced by space charge}}{\text{space-averaged electric field}}$$

$$\mathrm{Re} = \frac{\rho u_0 d}{\mu} = \frac{\text{inertia force}}{\text{viscous force}}$$

$$\mathrm{N}_{\mathrm{EHD}} = \frac{\rho_{c0} V_0}{\rho u_0^2} = \frac{\text{electrostatic body force}}{\text{inertia force}}$$

$$\Omega_0 = \frac{w_0}{u_0} = \frac{\text{space-averaged electrical migration velocity}}{\text{bulk gas velocity}}$$

$$\mathrm{Pe}_0 = \frac{w_0 d}{D_0} = \frac{\text{electrical convection of particle phase}}{\text{turbulent diffusion of particle phase}}$$

where $w_0 \equiv B_e E_0$ and the electrical drift parameter Ω_0 may be expressed as $\mathrm{De}_0\mathrm{Asp}$. The Deutsch number (Deutsch, 1922) De_0 means the dimensionless precipitator length, and Asp ($\equiv d/L$) is the aspect ratio. Consequently, the electrical potential, space charge density, EHD flow, and particle behavior inside the ESP depend on the five dimensionless parameters.

3. Results

3.1 Electrical characteristics

The distributions of electric field and space charge density are governed by the electrical parameter Y_0. So, first of all, the value of electrical parameter must be chosen to calculate the nondimensional electric field and space charge density. The experimental space charge densities at the corona wire in Fig. 2 is calculated from the experimental data of the voltage-current characteristics that have been cited from Park and Kim (2001). The map of Y_0 is plotted on the basis of the electrical characteristics of the present model ESP. The electrical characteristics may be changed by the operating conditions of ESPs or the gas conditions, such as the diameter or shape of discharge electrode, the contaminated situation of the collecting electrode by the deposited dust layer, the temperature, pressure, humidity,

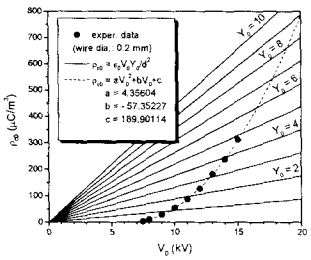

Figure 2. Electrical characteristics between the applied voltage and the space charge density at the corona wire.

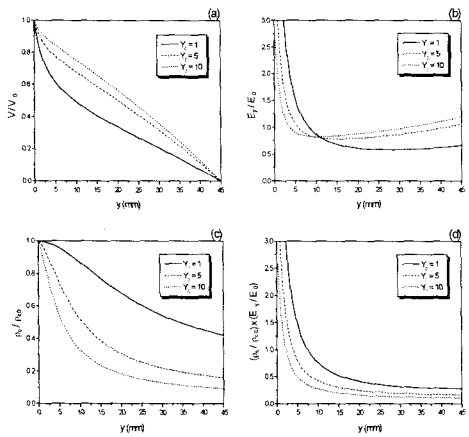

Figure 3. Normalized (a) electrical potential, (b) y-directional electric field strength, (c) space charge density, and (d) y-directional electrical body force strength along the symmetry line from corona wire to wall for the various space charge parameters.

or component of gas, or the mass loading of particles (Böhm, 1982). Therefore, we can select artificially the constant value of Y_0 for different corona voltages.

Figures 3 and 4 show the normalized distributions of the electrical potential and electric field strength, space charge density, and electrical body force along the normal distance from corona wire to wall surface for the various electrical parameters. It must be noticed that the electrical potential and space charge density are normalized by the values at corona wire and the electric field strength is normalized by the space-averaged electric field E_0 ($\equiv V_0 / d$). The large value of Y_0 at the same value of V_0 means that the space charge density is high in ESPs. Figure 3a shows that the electrical potential increases over the entire domain as the electrical parameter increases. Therefore the electric field strength decreases in vicinity of the discharge wire and increases near the grounded plate. The high electric field strength makes the current of ions near the ground electrode speedy, so that the profile of the normalized space charge density is steeper. And the normalized space charge density near the ground electrode becomes lower for increasing Y_0 as shown in Fig. 3c. As a result, the dimensionless electrical body force decreases as the electrical parameter increases as shown in Fig. 3d.

3.2 Electrohydrodynamic flow

The laminar EHD flow may be explained with the Reynolds number and EHD number only. However, the turbulent flow also depends on the electrical Peclet number and Deutsch number because the turbulent

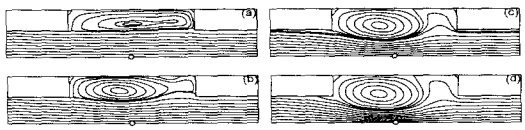

Figure 4. Electrohydrodynamic flow for various EHD numbers at Re = 1490, Y_0 = 1, Pe_0 = 100 and De_0 = 1; (a) N_{EHD} = 1, (b) N_{EHD} = 9, (c) N_{EHD} = 25, and (d) N_{EHD} = 49.

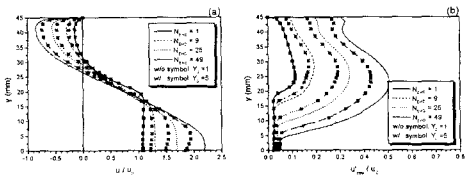

Figure 5. Normalized x-directional (a) gas mean velocity and (b) turbulence intensity profiles along the sysmmetry line from corona wire to wall for various EHD numbers at Y_0 = 1 and 5, Re = 1490, Pe_0 = 100, and De_0 = 1.

fluctuation velocity is connected with the turbulent diffusivity of the particle phase. The range of EHD number is from zero without the corona discharge to infinity without the inlet cross-flow. We have selected the EHD number values from 0.25 to 49.

Figure 4 illustrates the variation of EHD flow with the different EHD number N_{EHD} for Re = 1490, Y_0 = 1, Pe_0 = 100 and De_0 =1. The circulatory cell plumps gradually and the circulating flow intrudes into the cross-flow region as the EHD number increases. The streamline entering the ESP via the inlet wall surface does not invade deeply into the cavity for N_{EHD} = 1 and 9. However, the streamline is deflected toward the centerline of ESP and then approaches the upper wall surface of the cavity by the intense corona wind for N_{EHD} = 25 and 49. The EHD flow field becomes slightly different when the electrical parameter Y_0 increases. As the electrical parameter increases, the increasing rate of gas velocity induced by the corona wind decreases. This is because the dimensionless electrical body force is reduced with Y_0, as explained in Fig. 3d. Also, as the electrical parameter increases, the turbulence intensity decreases because the strength of the additional circulating flow caused by the corona wind is reduced (Fig. 5b). The EHD flow streamlines were hardly changed when the Reynolds number increases to be 2980. That is, the increase of Reynolds number does not influence the variation of EHD flow field under the operating condition of conventional ESPs.

The electrical Peclet number Pe_0 is a measure of the relative strengths of the electrical migration force and turbulent diffusion on the particle transport. Therefore

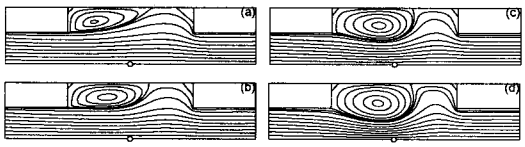

Figure 6. Electrohydrodynamic flow for various EHD numbers at Re = 2980, Y_0 = 5, Pe_0 = 1 and De_0 = 1: (a) N_{EHD} = 1; (b) N_{EHD} = 9; (c) N_{EHD} = 25; and (d) N_{EHD} = 49.

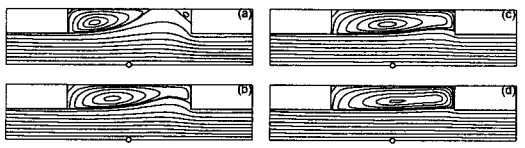

Figure 7. Electrohydrodynamic flow for various electrical Peclet numbers at Re = 2980, Y_0 = 5, N_{EHD} = 1 and De_0 = 1; (a) Pe_0 = 1; (b) Pe_0 = 5, (c) Pe_0 = 10, and (d) Pe_0 = 100.

the range of Pe_0 is from 0 to infinity. The limit $Pe_0 \rightarrow 0$ corresponds to the Deutsch model of complete mixing ($D_0 \rightarrow \infty$) while the limit $Pe_0 \rightarrow \infty$ corresponds to laminar flow ($D_0 \rightarrow 0$). In general, the collection efficiency of ESPs is from the prediction calculated from the Deutsch formula as lower limit to that calculated from the laminar flow assumption as upper limit. That is, the collection efficiency increases for increasing electrical Peclet number, i.e. for decreasing turbulent diffusivity D_0, in the conventional flat plate – plate and wire – flat plate ESPs. In the present study, the electrical Peclet numbers range from 1 to 1000, meaning that the turbulent diffusivities are from 50 to 0.05 cm^2/s when the space-averaged electrical migration velocity w_0 = 0.1 m/s and the wire-plate spacing d is 5cm. Those values are reasonable in conventional ESPs (Leonard *et al.*, 1982).

Figure 6 illustrates the EHD flow streamlines for Pe_0 = 1. Reminding that the EHD flow was hardly changed for increasing Reynolds number, we may compare the EHD flows changed significantly for decreasing electrical Peclet number at N_{EHD} = 1 and 9 while the strength of circulating flow is reduced slightly at N_{EHD} = 25 and 49. That is, the gas flow with high turbulence intensity entering the ESP influences considerably the flow field inside the ESP when the EHD number is low. Figure 7 shows the variation of EHD flow field with electrical Peclet number for N_{EHD} = 1. As the electrical Peclet number decreases, i.e. the turbulent fluctuating velocity of inlet cross-flow increases, the flow streamlines via the vicinity of inlet wall curve into the cavity region, so that the circulatory cell is reduced. This can be explained by the studies about the variation of reattachment length in the backward facing step flow with Reynolds number. The reattachment length increases with Reynolds number at the laminar flow regime (Denham and Patrick, 1974). However, the regime of transitional flow is characterized by a continued gradual, but irregular decrease to a minimum value at a Reynolds number, then an increase to a constant level that characterizes the turbulent flow regime (Armaly *et al.*, 1983). The flow condition of Fig. 7 is not included in the laminar and turbulent flow regimes both, corresponding with the operating conditions of conventional ESPs. Consequently, the inlet cross-flow curves into the cavity in the transitional flow regime, so that the more amounts of the particles entering the ESP may be entrapped into the cavity as the turbulent diffusivity of inlet cross-flow increases. Therefore, we can expect that the collection efficiency increases as the electrical Peclet number decreases.

3.3 Particle collection efficiency

Particle transport in the ESP is calculated on the basis of the computational results for the electric field and EHD flow field. As mentioned above, the convective

diffusion equation of particle phase depends on the electrical drift parameter and electrical Peclet number. The electrical drift parameter Ω_0 is a function of Deutsch number De_0. The Deutsch number means a measure of the electrical mobility of a particle when the geometry size, gas bulk velocity, and electric field are fixed. That is, the Deutsch number increases as the electrical migration velocity of particle increases. In the Deutsch formula (1922), the collection efficiency is 0.632 for the particles with $De_0 = 1$.

Figure 8 shows the particle collection efficiency versus EHD number for $Y_0 = 1$ and 5 at Re = 1490, $Pe_0 = 100$, and $De_0 = 0.5$. Because the electric field intensity increases over the entire domain of ESP except for the vicinity of corona wire as the electrical parameter Y_0 increases (Fig. 3b), the collection efficiency is larger for $Y_0 = 5$ than for $Y_0 = 1$. And the collection efficiency decreases and then increases, i.e. has a minimum value,

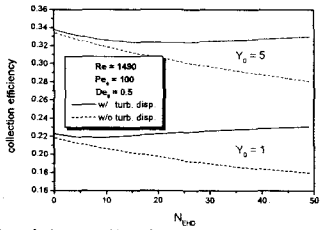

Figure 8. Particle collection efficiency versus EHD number for the different values of Y_0 at Re = 1490, $Pe_0 = 100$ and $De_0 = 0.5$.

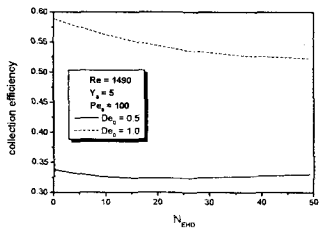

Figure 9. Particle collection efficiency versus EHD number for the different values of De_0 at Re = 1490, $Y_0 = 5$ and $Pe_0 = 100$.

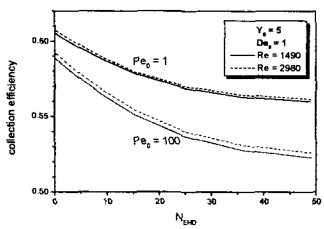

Figure 10. Particle collection efficiency versus EHD number for the different values of Pe_0 at Re = 1490, $Y_0 = 5$ and $De_0 = 1$.

as the EHD number increases. The decrease of efficiency may be explained by the streamline deflected toward the centerline of ESP shown in Fig. 4b. That is, the particles entering the ESP along the streamlines move toward the centerline of ESP, so that the particle transport into the cavity decreases. We introduced the convective diffusion model not considering the turbulent dispersion to estimate the effect of turbulent diffusion on the particle transport and collection efficiency. It was assumed that the particles are dispersed in the ESP by the Brownian diffusion only. The collection efficiencies calculated from the concentration profiles at the outlet of ESP are plotted as the dash lines. The collection efficiency decreases monotonically for increasing EHD number when the turbulent dispersion of particle phase is not considered. Consequently, the circulating flow due to the corona wind prevents the particle transport into the cavity.

However, when the Deutsch number is higher, i.e. the electrical mobility of particles is larger, the collection efficiency decreases monotonically for increasing EHD number, as shown in Fig. 9. Because a large number of particles with higher electrical mobility are transported into the cavity via the upstream part of cavity by the electrical migration for the low EHD number, the a lot of particles are not transported into the cavity by the streamline deflected toward the centerline of ESP as the EHD number increases. At $De_0 = 1$, the particle transport by the turbulent dispersion via the downstream part of cavity is happened for the high EHD number. However, the amounts of particles not transported into the cavity via the upstream part of cavity by the intense circulating flow are higher in comparison with the amounts of particles transported into the cavity by the turbulent dispersion. Therefore, the collection efficiency of particles with higher electrical migration velocity decreases as the EHD number increases. And the phenomenon like this is also occurred when the electrical Peclet number becomes lower (i.e. the turbulent diffusivity of inlet flow becomes higher).

Figure 10 shows that the particle collection efficiency decreases as the EHD number increases for $Pe_0 = 1$ and 100. The collection efficiency is higher and the decreasing rate of efficiency is lower for $Pe_0 = 1$ than for $Pe_0 = 100$. The former is because the cross-flow with high turbulent fluctuation curves deeply into the cavity and the turbulent fluctuation promotes the particle transport into the cavity. And the latter is because the circulating flow due to the corona wind is depressed by the cross-flow with high turbulence intensity and the high turbulent fluctuation of cross-flow increases the particle transport into the cavity. Also, Fig. 10 shows that the difference of collection efficiency with Reynolds number is insignificant.

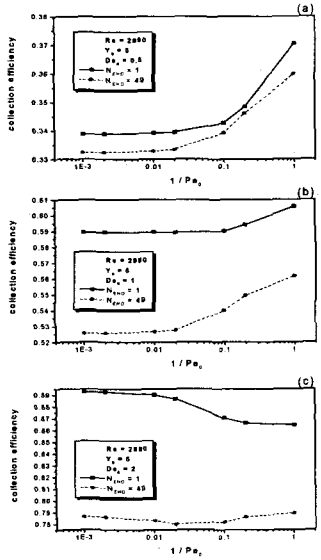

Figure 11. Particle collection efficiency versus electrical Peclet number for the different values of N_{EHD} at Re = 2980 and Y_0 = 5; (a) De_0 = 0.5, (b) De_0 = 1, and (c) De_0 = 2.

Figure 11 shows the particle collection efficiency versus the electrical Peclet number with N_{EHD} = 1 and 49 for De_0 = 0.5, 1, and 2. For De_0 = 0.5 and 1, the collection efficiency increases as the electrical Peclet number decreases. This is because the streamlines of inlet cross-flow curve into the cavity and the particles are dispersed in the cavity by the intense turbulent fluctuation for N_{EHD} = 1. For N_{EHD} = 49, the efficiency increases for decreasing electrical Peclet number because the circulating flow due to the corona wind is reduced by the cross-flow with high turbulence intensity and the particles are dispersed into the cavity by the intense turbulent fluctuation of cross-flow.

4. Conclusion

The effects of the EHD flow caused by corona wind and the turbulence condition of inlet cross-flow on the particle transport inside a wire – cavity plate ESP and the collection efficiency were studied through the computational analysis. The governing equations for the electric field, gas flow field, and particle concentration field were nondimensionalized, so that the five dimensionless parameters were derived.

As the space charge increased, the electrical potential increased over the entire domain of ESP, so that the electric field strength decreased near the corona wire and increased near the collecting plate. The ions generated by the corona discharge influenced significantly the flow field in the ESP. As the ratio of the electrostatic body force of ions to the inertia force due to the cross-flow convection increased, the strength of EHD circulating flow was enhanced in the ESP. When the electrostatic body force was predominant, the streamline via the inlet wall surface was deflected toward the centerline of ESP and then reattached to the bottom wall of the cavity. And the circulating flow was reduced as the turbulence level of inlet cross-flow increased. When the turbulence level of cross-flow was very high for the weak EHD flow, the streamlines through the inlet of ESP curved into the cavity, therefore the particle transport into the cavity increased. When the electrostatic body force of ions was weak, the EHD flow was affected significantly by the turbulence condition of inlet cross-flow. However, the cross-flow with high turbulent fluctuation did not influence significantly the EHD flow field inside the ESP when the electrostatic body force was strong.

As the ion space charge increased, the particulate collection efficiency increased because the electric field strength increased over the entire domain in the ESP except for the vicinity of corona wire. And the collection efficiency decreased and then increased, i.e. had a minimum value, as the EHD circulating flow became stronger when the electrical migration velocity of particle was low. On the other hand, the collection efficiency decreased for the stronger EHD flow when the electrical migration of particle was higher relatively. And the collection efficiency of a wire – cavity plate ESP increased as the turbulence level of inlet cross-flow increased when the electrical migration velocity of particle was low. However, the collection efficiency decreased for increasing the turbulent fluctuation of cross-flow when the electrical migration of particle was higher relatively.

Reference

(1) Armaly, B.F., Durst, F., Pereira, J.C.F. and Schönung, B., 1983, "Experimental and theoretical investigation of backward-facing step flow," *J. Fluid Mech.* Vol. 127, pp. 473~496.

(2) Böhm, J., 1982, *Electrostatic precipitators*, Chemical Engineering Monographs Vol.14, ELSEVIER Scientific Publishing Company, New York, 1982.

(3) Denham, M.K. and Patrick, M.A., 1974, "Laminar flow over a downstream-facing step in a two-dimensional flow channel," *Trans. Inst. Chem. Engrs.* Vol. 52, p. 361.

(4) Deutsch, W., 1922, *Ann. Phys.* Vol. 68, pp. 335~344.

(5) Elghobashi, S., 1994, "On predicting particle-laden turbulent flows," *Applied Sci. Research* Vol. 52, pp. 309~329.

(6) Kallio, G.A. and Stock, D.E., 1992, "Interaction of

electrostatic and fluid dynamic fields in wire-plate precipitators," *J. Fluid Mech.* Vol. 240, pp. 133~166.
(7) Leonard, G.L., Mitchner, M. and Self, S.A., 1982, "Experimental study of the effect of turbulent diffusion on precipitator efficiency," *J. Aerosol Sci.* Vol. 11, pp. 271~284.
(8) Riehle, C. and Löffler, F., 1995, "Grade efficiency and eddy diffusivity models," *J. Electrostatics* Vol. 34, pp. 401~413.
(9) Yabe, A., Mori, Y. and Hijikata, K., 1978, "EHD study of the corona wind between wire and plate electrodes," *AIAA J.* Vol. 16, pp. 340~345.
(10) Yamamoto, T. and Velkoff, H.R., 1981, "Electrohydrodynamics in an electrostatic precipitator," *J. Fluid Mech.* Vol. 108, pp. 1~18.